Posted on 24 Jan 2023 — The copyright holder is the author/funder. All rights reserved. No reuse without permission. — https://doi.org/10.22541/au.167458073.32400363/v1 — This a preprint and has not been peer reviewed. Data may be preliminary.

SARS-CoV-2 papain-like protease inhibits IL-1β maturation and pyroptosis through disruption of ASC oligomerization and deubiquitination of ASC

Huan Meng[1], Jianglin Zhou[2], Xiaojuan Chen[2], MingYu Wang[2], Mei Zheng[1], Yunhui Li[1], Ying Han[1], Jin Chen[1], Jinyu Han[1], Jing Liang[1], Yaling Xing[2], and Yajie Wang[1]

[1]Capital Medical University
[2]Beijing Institute of Microbiology and Epidemiology

January 24, 2023

Abstract

The perplexing innate immune response induced by SARS-CoV-2 infection remains inadequate uncovered. Previous studies showed that coronavirus papain-like protease (PLP) could evade type I interferons mediated innate immune responses. In this study, we found the inflammasome genes (NLRP3, NLRP6, PYCARD, IL1B, IL18, TRIM31, FBXL2, MARCH7) were down-regulated in CD14+ monocytes from COVID-19 patients. Secondly, we found that SARS-CoV-2 PLP may act on the NLRP3 inflammasome pathway. PLP may interact with ASC and interrupt ASC oligomerization by reducing the K48-linked and K63-linked ubiquitination of ASC, so that the excessive activation of the NLRP3 inflammatory pathway might be inhibited and the release of IL-1β was blocked. Thirdly, SARS-CoV-2 PLP negatively regulated the pyroptosis of host cells, which was mediated by caspase-1, the key regulator of the NLRP3 inflammasome pathway. In general, SARS-CoV-2 PLP avoids the excessive immune defenses in the early stage of virus infection, which provides the maximum advantage for virus replication. These insights uncover the flex function of CoV encoding proteases. Furthermore, this research may provide a new vision of COVID-19 epidemic prevention and new possibilities for new therapies.

ΣΑΡΣ-ὃ″-2 παπαιν-λικε προτεασε ινηιβιτς ΙΛ-1β ματυρατιον ανδ πψροπτοσις τηρουγη δισρυπτιον οφ ΑΣ‴ ολιγομεριζατιον ανδ δευβιχυιτινατιον οφ ΑΣ‴

Huan Meng[1, 2, #], Jianglin Zhou[2, #], Xiaojuan Chen[2], MingYu Wang[2], Mei Zheng[1], Yunhui Li[1], Ying Han[1], Jin Chen[1], Jinyu Han[1], Jing Liang[1], Yaling Xing[2, *], Yajie Wang[1,*]

1 Department of Clinical Laboratory, Beijing Ditan Hospital, Capital Medical University, Chaoyang District, Beijing 100015, China

2 Beijing Institute of Microbiology and Epidemiology, Beijing, 100850, China.

*** Correspondence: yalingxing@126.com, wangyajie@ccmu.edu.cn**

 # Huan Meng and Jianglin Zhou contributed equally to this work.

ΣΑΡΣ-ὃ″-2 παπαιν-λικε προτεασε ινηιβιτς ΙΛ-1β ματυρατιον ανδ πψροπτοσις τηρουγη δισρυπτιον οφ ΑΣ‴ ολιγομεριζατιον ανδ δευβιχυιτινατιον οφ ΑΣ‴

Abstract

The perplexing innate immune response induced by SARS-CoV-2 infection remains inadequate uncovered. Previous studies showed that coronavirus papain-like protease (PLP) could evade type I interferons mediated

Posted on 24 Jan 2023 — The copyright holder is the author/funder. All rights reserved. No reuse without permission. — https://doi.org/10.22541/au.167458073.32400363/v1 — This a preprint and has not been peer reviewed. Data may be preliminary.

innate immune responses. In this study, we found the inflammasome genes (NLRP3, NLRP6, PYCARD, IL1B, IL18, TRIM31, FBXL2, MARCH7) were down-regulated in CD14+ monocytes from COVID-19 patients. Secondly, we found that SARS-CoV-2 PLP may act on the NLRP3 inflammasome pathway. PLP may interact with ASC and interrupt ASC oligomerization by reducing the K48-linked and K63-linked ubiquitination of ASC, so that the excessive activation of the NLRP3 inflammatory pathway might be inhibited and the release of IL-1β was blocked. Thirdly, SARS-CoV-2 PLP negatively regulated the pyroptosis of host cells, which was mediated by caspase-1, the key regulator of the NLRP3 inflammasome pathway. In general, SARS-CoV-2 PLP avoids the excessive immune defenses in the early stage of virus infection, which provides the maximum advantage for virus replication. These insights uncover the flex function of CoV encoding proteases. Furthermore, this research may provide a new vision of COVID-19 epidemic prevention and new possibilities for new therapies.

Key words: SARS-CoV-2; papain-like protease; NLRP3 inflammasome; IL-1β· pyroptosis; ASC; deubiquitination

Introduction

Since the 2019 coronavirus disease (COVID-19) pandemic caused by the human severe acute respiratory syndrome coronavirus-2 (SARS-CoV-2) began at the end of 2019, there have been over 650 million confirmed cases of COVID-19 and over 6.6 million deaths [1], which showed a serious impact on human health and life.

As SARS-CoV-2 invaded the organism, the immune system would respond to the virus invasion and induce complex pathology in hosts. The innate immune system, as the first line of defense against SARS-CoV-2, plays a vital role in the clearance of viruses [2]. Infected cells may prime the innate immune response to clear the virus in the early stages of infection; however, SARS-CoV-2 may evade the type I innate immune response mediated by type I interferons (IFN) and pro-inflammatory cytokines like IL-1, IL-6, and TNF in multiple ways, contributing to early viral replication and spread[3,4].

Papain-like protease (PLP) is one of the domains included by coronavirus's non-structural protein 3 (nsp3), which exhibits catalytic activity in processing the cleavage of nsp1—nsp2, nsp2—nsp3, and nsp3—nsp4 and shows de-ubiquitination activity. In addition, PLP participates in virus replication in collaboration with other proteases like the main protease 3CL [5]. Previous studies in our laboratory showed that the NL63 PLP2-mediated IFN antagonistic component[6]. Membrane-associated PLP (PLP-TM) of NL63 or SARS inhibited STING-mediated nuclear translocation activation of IRF-3 and promoter-dependent induction of IRF-3, which also negatively regulated the assembly of the STING-MAVS-TBK1/IKK complex required for IRF-3 activation, thereby inhibited IFN expression [7,8]. Moreover, MERS PLP also antagonizes IFN-mediated immune responses. CoV PLP interacts with Beclin-1 to induce incomplete autophagy and thus impedes antiviral innate immunity [9]. Recent research elaborates that SARS-CoV-2 PLP shows deISGylating activity and lower catalytic activity on K48-linked Ub chains compared with SARS-CoV PLP[10-12]. What's more, as with SARS PLP and MERS PLP, SARS-CoV-2 PLP also attenuates IFN-mediated immunity and regulates the replication and spread of the virus [13].

IFN and pro-inflammatory cytokines like IL-1β play essential roles in engaging innate immune defenses. The NLRP1, NLRP3, IPAF, and AIM2 inflammasomes are common platforms for the maturation of IL-1β and induce pyroptosis [14]. Different from other inflammasomes, the NLRP3 inflammasome could be stimulated by a wide variety of activators, such as the single-strand virus[15]. The NLRP3 inflammasome is composed of three key molecules: the NACHT, LRR, and PYD domains-containing protein 3 (NLRP3), the adaptor apoptosis-associated speck-like protein containing a caspase recruitment domain (ASC), and pro-caspase-1. With the right stimuli, these three molecules could form a complex that further acts on downstream pro-inflammatory cytokines such as IL-1β and induce pyroptosis [14].

As SARS-CoV-2 PLP has been reported to inhibit IFN-mediated innate immunity [13], we suspect that SARS-CoV-2 PLP would impact the NLRP3 inflammasome pathway. This article pays attention to SARS-CoV-2 PLP interacting with the NLRP3 inflammasome pathway.

Posted on 24 Jan 2023 — The copyright holder is the author/funder. All rights reserved. No reuse without permission. — https://doi.org/10.22541/au.167458073.32400363/v1 — This a preprint and has not been peer reviewed. Data may be preliminary.

2 Materials and methods

2.1 Reagents

Dulbecco's Modified Eagle Medium (gibco, C11995500BT), RIMP-1640 (SIGMA, R8758-500ML), FBS (Beyotime, C0234), Lipopolysaccharides from Escherichia coli O55:B5 (SIGMA, 12190801), nigericin (invivogen, tlrl-nig), Phorbol 12-myristate 13-acetate (PMA) (SIGMA, P1585-10mg), disuccinimidyl suberate (DSS) (Thermo Fisher Scientific, A39267), IL-1β ELISA kit (Dakewe, 1110122), Anti-DDDDK-tag mouse mAb (MBL, M185-3L), Anti-Myc-tag mouse mAb (MBL, M192-3), Anti-HA-tag mouse mAb (MBL, M180-3), Anti-Myc-tag rabbit pAb (MBL, 562), NLRP3 (D4D8T) Rabbit mAb (CST, 15101S), V5-Tag (D3H8Q) Rabbit mAb (CST, 13202S), Cleaved-IL-1β (Asp116) (D3A3Z) Rabbit mAb (CST, 83186S), IL-1β (D3U3E) Rabbit mAb (CST, 12703S), ASC/TMS1 (E1E3I) Rabbit mAb (CST, 13833S), Caspase-1 (D7F10) Rabbit mAb (CST, 3866), Gasdermin D (E8G3F) Rabbit mAb (CST, 97558S), Cleaved Caspase-1 (Asp297) (D57A2) Rabbit mAb (CST, 4199S), Anti-cleaved N-terminal GSDMD antibody [EPR20829-408] (Abcam, ab215203), β-Actin Rabbit mAb (High Dilution) (ABclonal, AC026), Anti-IgG (H+L chain) (Mouse) pAb-HRP (MBL, 330), Anti-IgG (H+L chain) (Rabbit) pAb-HRP (MBL, 458), Protein A + G agarose (Beyotime, P2012), lipofectamine 2000 reagent (Invitrogen, 11668-019), CellTiter-Glo luminescent cell viability assay kit (Promega, G7570), CytoTox 96 non-radioactive cytotoxicity assay kit (Promega, G1780), protease inhibitor cocktail (Beyotime, P1005), DAPI (Beyotime, C1002), Antifade Mounting Medium (Beyotime, P0126-5ml), Alexa Fluor® 594-labeled goat anti-rabbit IgG (H+L) (Affinity purified) (ZSGB-BIO, ZF-0516), Alexa Fluor® 594 Goat Anti-Mouse IgG (H+L) (Affinity Purified) (ZSGB-BIO, ZF-0513), Alexa Fluor® 488 Polyclonal Goat Anti-Rabbit IgG (H+L) (ZSGB-BIO, ZF-0511), Cy5 conjugated Goat Anti-mouse IgG (H+L) (Servicebio, GB27301), glass bottom cell culture dish (NEST, 801002).

2.2 Data collection and reanalysis

The raw scRNA-seq FASTQ files of PBMCs were downloaded from the Genome Sequence Archive of the Beijing Institute of Genomics (BIG) Data Center (HRA000150). These reads were then parsed by Cell Ranger (v.4.0.0) count pipeline with the GRCh38 human reference genome to generate gene expression matrices respectively. The subsequent analyses were performed by R (v.4.0.2) scripts with Seurat (v.3.2.2) package. Eight genes (NLRP3, NLRP6, PYCARD, IL1B, IL18, TRIM31, FBXL2, MARCH7) were used to define the Inflammasome pathway score. All of the boxplots in this study were plotted using "geom_boxplot" in ggplot2 (ggplot2: Elegant Graphics for Data Analysis. Springer-Verlag New York, 2016) R package. Wilcoxon rank-sum test was applied to test the significance of the difference between conditions using the "geom_signif" function in ggsignif (Significance Brackets for 'ggplot2') R package. The analysis method can be consulted in the supplementary material

2.3 Cell culture and stimulation

HEK-293T cells and BEAS-2B cells were cultured in Dulbecco's modified Eagle's medium (DMEM) supplemented with 10%FBS and 1% P/S, THP-1 cells purchased from National Infrastructure of Cell Line Resources (NICR) were cultured in RIMP-1640 supplemented with 10%FBS and 1% P/S at 37 under 5% CO2. THP-1 cells were differentiated into macrophages by treatment with 20ng/ml PMA for 36h. THP-1 macrophages were then stimulated with 1ug/ml LPS for 3h followed by 10μM nigericin for 3h. BEAS-2B cells were stimulated with 10ug/ml LPS for 12h followed by 10μM nigericin for 3h. Cell lysates were collected for western blotting, supernatants were collected for ELISA.

2.4 Plasmids construction and transfection

SARS-CoV-2 PLP-TM (aa 1564 – aa 2394 of pp1ab) was encoded into V5/HisB vector between Myc-NLRP3, Myc-ASC, and Myc-pro-caspase-1 were gift kingly provided by Jian Wang (Beijing Proteome Research Center, China). ASC was cloned into pcDN3.1 HA-tagged vector/Flag-tagged vector (obtained from miaolingbio) between Hind III and EcoR I. The cDNAs encoding human pro-IL-1β were obtained by reverse transcription of total RNA from THP-1 macrophages, followed by PCR using specific primers. According to the operation manual, Lipofectamine 2000 was used to transfect plasmids into cells.

Posted on 24 Jan 2023 — The copyright holder is the author/funder. All rights reserved. No reuse without permission. — https://doi.org/10.22541/au.167458073.32400363/v1 — This a preprint and has not been peer reviewed. Data may be preliminary.

2.5 Lentivirus production and infection

GFP-Flag-PLP-TM-Lentivirus and GFP-CT-Lentivirus (control vector) were constructed by genechem (Shanghai). 5E+8 TU/ml GFP-Flag-PLP-TM-Lentivirus or 1E+8 TU/ml GFP-CT-Lentivirus infected THP-1 cells for 48h, and then infected THP-1 cells were cultured with 2.5ug/ml puromycin for 72h.

2.6 Co-IP assay

Plasmids were transfected into HEK-293T cells as indicated for 24h. Cells were lysed by NP-40 lysis buffer (50mmol/L Tris-HCl pH 7.4, 150mmol/L NaCl, 2mmol/L NaCl, 2mmol/L EDTA, 1% NP-40) containing protease inhibitor cocktail (Beyotime, 1mmol/L). Protein was immunoprecipitated with Protein A/G agarose beads (Beyotime) and proper antibody. Collecting the precipitate and adding 50ul 2×loading buffer to end the reaction. Finally, Western blotting was used to detect the interaction between two proteins.

2.7 Co-IP Ubiquitination assay

Plasmids were transfected into HEK-293T cells as indicated for 24h. Then cells were cultured with 25mmol/L MG-132 for 4h. Cells were lysed by RIPA buffer (50mmol/L Tris-HCl pH 7.4, 150mmol/L NaCl, 2mmol/L NaCl, 2mmol/L EDTA, 1% NP-40, 0.1% SDS) containing protease inhibitor cocktail (Beyotime, 1mmol/L) and 10μmol/L NEM. Protein was immunoprecipitated with Protein A/G agarose beads (Beyotime) and proper antibody. Collecting the precipitate and adding 50ul 2×loading buffer to end the reaction. Finally, Western blotting was used to detect the interaction between two proteins.

2.8 Immunofluorescence

Cells were cultured in a glass bottom cell culture dish (NEST, 801002). The cells were fixed with 4% polyformaldehyde for 20min and incubated with 0.2% Triton X100 for 20min followed by 5% BSA for 1h, then the cells were incubated with indicated proper antibodies. The nucleus was dyed with DAPI for 5min. Finally, cells were covered with an anti-quenching agent. Images and three-dimension reconstruction were acquired by confocal microscope (Dragonfly, Andor). Image processing was conducted by Imaris Viewer 9.8.0.

2.9 Cell viability assay and Cytotoxicity assay

THP-1 cells were planted in 96-wells plates and stimulated as indicated, while BEAS-2B cells were planted in 96-wells plates and transfected with V5/HisB SARS-CoV-2 PLP-TM or vector for 24h, then BEAS-2B cells were stimulated with 10ug/ml LPS for 12h following with nig 10μM for 3h. The supernatants were collected for Lactate dehydrogenase (LDH) detection to assess cell death by using to assess cell death using a CytoTox 96 non-radioactive cytotoxicity assay kit (Promega). While the pellets were collected for cellular ATP determination to assess cell viability by using CellTiter-Glo luminescent cell viability assay kit (Promega).

2.10 ASC oligomerization

THP-1 macrophages were primed with LPS (1 ug/ml) for 3 h followed by 3 h nigericin (10 μmol/L) stimulation. ASC oligomerization assays were performed as previously described [16].

2.11 ΙΛ-1β μεασυρεδ βψ ΕΛΙΣΑ

IL-1β levels were measured by ELISA kit (1110122, Dakewe, Shenzhen) following the manufacturer's instructions.

2.12 Statistical analysis

The sample size was not predetermined by any statistical methods. Experiments were independently repeated at least three times to achieve statistical significance. Data were shown as means ± SD of three technical replicates. Data were analyzed by two-tailed Student's t-tests if not specified. GraphPad Prism 9.0 was used to analyze data.P -values < 0.05 were termed as significant ($^*P< 0.05$; $^{**}P < 0.01$; and $^{***}P< 0.001$); NS means non-significant.

3 Results

Posted on 24 Jan 2023 — The copyright holder is the author/funder. All rights reserved. No reuse without permission. — https://doi.org/10.22541/au.167458073.32400363/v1 — This a preprint and has not been peer reviewed. Data may be preliminary.

3.1 The inflammasome pathway is downgraded in the innate immune cells of COVID-19 patients

Previous studies showed that, compared with healthy donors, IL-1β levels in serum from COVID-19 patients were not elevated [17]. To figure out the cause of this phenomenon, we reanalyzed the single-cell RNA sequencing data (accession code HRA000150). PBMCs from 5 healthy donors, 11 COVID-19 patients (among them, there were 7 moderate patients and 4 severe patients), and 6 convalescent patients were collected for single-cell transcriptional sequencing. When analyzing, eight genes (*NLRP3, NLRP6, PYCARD, IL1B, IL18, TRIM31, FBXL2, MARCH7*) were used to define the inflammasome pathway score among natural killer cells, $CD14^+$ monocytes, $CD16^+$ monocytes, mononuclear dendritic cells, and dendritic cells. Compared with healthy donors and convalescent patients, the inflammasome pathway score was downgraded among $CD14^+$ mononuclear cells, mononuclear dendritic cells, and dendritic cells (Figure 1A). Furthermore, the expression levels of NLRP3, NLRP6, IL-1β, and MARCH7 fell in COVID-19 patients, while they rose again in convalescent patients (Figure 1B). These results indicated that the NLRP3-associated inflammasome pathway was downregulated in SARS-CoV-2-infected innate immune cells.

3.2 ΣΑΡΣ-ὃ″-2 ΠΛΠ ινηιβιτς ςασπασε-1 ςλεααγε ανδ ματυρατιον οφ ΙΛ-1β (π17)

As we observed that the expression levels of NLRP3/IL-1β were down-regulated in innate immune cells from COVID-19 patients, we want to further explore which protein encoded by the SARS-CoV-2 genome is involved in the down-regulated NLRP3 inflammasome pathway. A previous study has proven that SARS-CoV-2 PLP negatively regulates IFN-mediated innate immunity[13]. As our group has already reported, the negative regulation of IFNβ by other coronavirus PLPs[6,8,9], we suspected whether the SARS-CoV-2 PLP would inhibit the NLRP3 inflammasome to a certain extent. According to previous reports, the expression of PLP, including the downstream transmembrane (TM) domains, was required for processing at the cleavage sites in the polyprotein 1a (1ab) [18,19]. Whereupon, we constructed SARS-CoV-2 PLP-TM (aa 1564 – aa 2394 of pp1ab) into a V5/HisB-tagged plasmid (Figure S2). Then plasmids encoding NLRP3, ASC, pro-caspase-1, pro-IL-1β, and V5/HisB tagged SARS-CoV-2 PLP-TM were co-transfected into HEK-293T cells. The results showed that the expression levels of IL-1β (p17) in cell lysates and the secretion of IL-1β were decreased by SARS-CoV-2 PLP-TM (Figure 2A). In addition, we generated the THP-1 cells stably expressing Flag-tagged SARS-CoV-2 PLP-TM. After stimulation, the expression levels of IL-1β (p17) in cell lysates and supernatants were compared between the Flag-tagged SARS-CoV-2 PLP-TM -overexpressing cells and the control cells. The secretion of IL-1β (p17) in the Flag-tagged SARS-CoV-2 PLP-TM-overexpressing cells was less than in the control cells (Figure 2B). What's more, we also examined the expression of NLRP3 inflammasome adapting proteins. Among these proteins, cleaved caspase-1 (p20) was inhibited by SARS-CoV-2 PLP-TM (Figure 2B). The same phenomenon was also observed in BEAS-2B cells (Figure S3). Taken together, these results indicate that SARS-CoV-2 PLP-TM inhibits the activation of the NLRP3 inflammasome.

3.3 SARS-CoV-2 PLP inhibits GSDMD-mediated pyroptosis in THP-1 macrophages

The activation of the NLRP3 inflammasome recruits pro-caspase-1 and induces pro-caspase-1 to self-cleave. Then, the formation of cleaved-caspase-1 (p20) cuts GSDMD into two forms—GSDMD-N and GSDMD-C. GSDMD-N fuses into the membrane, and then the formation of membrane pores eventually causes cell swelling, which was thought to be the signature of cell pyroptosis[20]. Based on the findings above, we discovered that SARS-CoV-2 PLP-TM inhibited cleaved caspase-1 (p20) (Figures 2A-2B). As a result, we further observed the effect of SARS-CoV-2 PLP-TM on cell pyroptosis. Lipopolysaccharide (LPS) and nigericin were used to induce THP-1 pyroptosis, then the lactate dehydrogenase (LDH) releasing assay was conducted to reflect the cell death, and the cell viability assay was monitored by calculating ATPs in living cells. Compared with the control cells, SARS-CoV-2 PLP-TM-overexpressing THP-1 macrophages showed less cell cytotoxicity and more cell viability (Figures 3B–3C). Besides, the expression levels of GSDMD-N decreased in SARS-CoV-2 PLP-TM-overexpressing THP-1 macrophages (Figure 3A), however, all these results were only detected in THP-1 macrophages. In BEAS-2B cells, even though GSDMD-N (43 KDa) was inhibited by SARS-CoV-2 PLP-TM (Figure S4A), the cell death showed no differences between SARS-CoV-2 PLP-TM and the control cells (Figure S4B). These results in THP-1 macrophages were different from those

Posted on 24 Jan 2023 — The copyright holder is the author/funder. All rights reserved. No reuse without permission. — https://doi.org/10.22541/au.167458073.32400363/v1 — This a preprint and has not been peer reviewed. Data may be preliminary.

in BEAS-2B cells, as we found that GSDMD-N (43 KDa) expressed much higher than GSDMD-N (30 KDa) after stimulation with LPS and nig in BEAS-2B cells (Figure S4A). Another study showed that GSDMD can be cleaved at the 43 KDa site by caspase-3, which blocks pyroptosis[21]. We suspect that even though the NLRP3 inflammasome is activated by LPS and nig in BEAS-2B, the expression levels of caspase-3 might be stimulated much more than caspase-1. Altogether, these results reflect that SARS-CoV-2 PLP-TM might inhibit GSDMD-mediated pyroptosis in THP-1 macrophages.

3.4 SARS-CoV-2 PLP partially co-localizes with ASC

To visually observe the sub-cellular localizations of SARS-CoV-2 PLP-TM, NLRP3, pro-caspase-1, and ASC, HEK-293T cells were transfected with V5-SARS-CoV-2 PLP-TM, Myc-NLRP3, Myc-pro-caspase-1, and HA-ASC. The images of immunofluorescence were shot by confocal microscopy. As in other studies [22], NLRP3 was diffusely distributed in the cytoplasm (Figure 4A); pro-caspase-1 was diffusely distributed in the nucleus and cytoplasm (Figure 4A); ASC has two forms, one of which was diffusely distributed in the nucleus and cytoplasm, and the other form of which was organized into specks in the cytoplasm (Figure 4A). After stimulation, ASC was redistributed from the nucleus to the cytoplasm and formed specks [23]. While in THP-1 macrophages, ASC distributed in the nucleus and the cytoplasm without stimulation, but when cultured with LPS and nigericin, ASC formed specks in the cytoplasm (Figure 4D, Figure 4E), which is the same as the research reported previously [24].

In this research, we constructed two transmembrane domains—TM1 and TM2 along with PLP. PLP could locate on the ER membrane in the presence of TM1 and TM2 [5], so we observed that SARS-CoV-2 PLP-TM mainly spread in the cytoplasm (Figure 4A). When NLRP3/ASC/pro-caspase-1 were separately co-transfected with SARS-CoV-2 PLP-TM, no co-localizations of SARS-CoV-2 PLP-TM with NLRP3 or pro-caspase-1 were observed (Figure 4B), but ASC was partially co-localized with SARS-CoV-2 PLP-TM. Interestingly, in our experiment, when ASC specks formed, SARS-CoV-2 PLP-TM could constitute a 'ring-like' structure (Figure 4B). Compared with the control cells, SARS-CoV-2 PLP-TM might co-localize with ASC in the absence of stimulation; while after stimulation, SARS-CoV-2 PLP-TM formed the same structure as in HEK-293T cells (Figure 4D). To observe the 'ring-like' structure more entirely, we observed the three-dimensional structure through three-dimensional reconstruction by scanning slice by slice. Interestingly, the 'ring-like' SARS-CoV-2 PLP-TM could wrap around an ASC speck. To further study whether SARS-CoV-2 PLP-TM could damage the co-localization of NLRP3 with ASC, we constructed SARS-CoV-2 PLP-TM into GFP-tagged plasmids and transfected them with Myc-NLRP3 and HA-ASC into HEK-293T cells. As observed, Myc-NLRP3 and HA-ASC could interact with each other and form a complex (Figure 4C), however, SARS-CoV-2 PLP-TM still formed a "ring-like" structure and wrapped around the complex (Figure 4C), which didn't change the NLRP3-ASC complex. All these results indicate that SARS-CoV-2 PLP-TM might co-localize with ASC and form a 'ring-like' structure to wrap ASC around. Thus, as to our observation, SARS-CoV-2 PLP-TM might not destroy the NLRP3-ASC complex, but might subsequently interrupt the form of the NLRP3-ASC-caspase-1 complex.

3.5 SARS-CoV-2 PLP binds with ASC

During the process of NLRP3 inflammasome activation, the formation of the NLRP3-ASC-caspase-1 complex is the key to inducing the maturation of IL-1β and the formation of GSDMD-N [15]. The upper results indicate that SARS-CoV-2 PLP-TM might inhibit the activation of the NLRP3 inflammasome and pyroptosis, however, we are still confused about how SARS-CoV-2 PLP-TM affects the activation of the NLRP3 inflammasome. Therefore, we detected the interaction between SARS-CoV-2 PLP-TM and NLRP3/ASC/caspase-1/pro-IL-1β separately by co-IP assay. As a result, we found that SARS-CoV-2 PLP-TM interacts with ASC (Figures 5A–5D). These results indicate that SARS-CoV-2 PLP-TM might interact with ASC so that it could inhibit the activation of the NLRP3 inflammasome and pyroptosis.

3.6 SARS-CoV-2 PLP interrupts the oligomerization of ASC

The oligomerization of ASC is an important sign in the activation of the NLRP3 inflammasome, while the formation of ASC oligomers is critical for inducing pro-caspase-1 cleavage. In HEK-293T cells, V5-

Posted on 24 Jan 2023 — The copyright holder is the author/funder. All rights reserved. No reuse without permission. — https://doi.org/10.22541/au.167458073.32400363/v1 — This a preprint and has not been peer reviewed. Data may be preliminary.

tagged SARS-CoV-2 PLP-TM plasmids were co-transfected with plasmids encoding NLRP3, ASC, and pro-caspase-1 for 24 h, then ASC oligomers were detected by immunoblotting. As we can see in Figure 6A, SARS-CoV-2 PLP-TM could inhibit the oligomerization of ASC. SARS-CoV-2 PLP-TM could reduce the ASC oligomers stimulated by LPS and nig in THP-1 macrophages (Figure 6B). What's more, the same results were observed in BEAS-2B cells (Figure S5). These results reflect that SARS-CoV-2 PLP-TM might inhibit the oligomerization of ASC when the NLRP3 inflammasome pathway was excessively activated.

3.7 SARS-CoV-2 PLP reduces K48-linked and K63-linked ubiquitination of ASC

Protein modification plays an important role in the activation of the NLRP3 inflammasome. Among these modifications, ubiquitination and deubiquitination are of great significance. While the deubiquitination of NLRP3 and ubiquitination of ASC, pro-caspase-1, and pro-IL-1β are required for the NLRP3 inflammasome activation [25,26]. In addition, SARS-CoV-2 PLP-TM as an enzyme has a Ub binding domain and could play a role in the deubiquitination of poly-Ub[27]. As a result, we investigated whether SARS-CoV-2 mediated deubiquitination of NLRP3, ASC, and pro-caspase-1. Plasmids encoding SARS-CoV-2 PLP-TM were transfected into HEK-293T cells together with plasmids encoding NLRP3 or ASC or pro-caspase-1 and ubiquitin. All these results showed that SARS-CoV-2 PLP-TM could reduce the ubiquitination of ASC (Figure 7A–7C). The result reminds us that SARS-CoV-2 PLP-TM might inhibit the activation of the NLRP3 inflammasome through involvement in the deubiquitination of ASC.

To further reveal the possible SARS-CoV-2 PLP-TM-mediated deubiquitination site of ASC. We transfected V5-tagged SARS-CoV-2 PLP-TM, Flag-ASC, and HA-tagged K48- or K63-linked ubiquitin into HEK-293T cells. Even though other research about SARS-CoV-2 PLP presents a poor ability to recognize K48- and K63-linked di-Ub, we still observed that SARS-CoV-2 PLP-TM could reduce both K48- and K63-linked ubiquitination of ASC (Figure 7D–7E). These results reflect the possibility that SARS-CoV-2 PLP-TM might reduce ASC's K48- and K63-linked ubiquitination.

4 Discussion

In this study, we found that the gene expression of NLRP3 and IL-1β was downregulated in CD14+ and CD16+ monocytes from COVID-19 patients, while MARCH7 and IL-18 declined only in CD16+ monocytes. Further studies show that SARS-CoV-2 PLP-TM might block IL-1β maturation, and subsequently inhibit the activation of GSDMD, reducing the release of IL-1β. Specifically, SARS-CoV-2 PLP-TM interacts with ASC and reduces the ASC's K48- and K63-linked ubiquitination, which decreases ASC's oligomerization and the formation of the NLRP3 inflammasome complex (Figure 8). The protease encoded by the SARS-CoV-2 genome interacting with host proteins to antagonize host antiviral immunity might explain why asymptomatic patients accounted for one-third of the total number of infected patients [28].

Like other coronaviruses, after infection into host cells, the SARS-CoV-2 genome starts to translate first and encodes two large polyproteins, pp1a and pp1ab, which contain non-structural proteins 1–16, while PLP plays a vital role in releasing nsp1-3 and regulating virus replication [29]. Furthermore, previous research has shown that SARS/NL63-CoV PLP functions as an innate immunity antagonist and plays a novel role in the viral immune escape, which may benefit virus replication.

In this research, we found SARS-CoV-2 PLP-TM could inhibit IL-1β maturation, which might explain why there was no significant increase in pro-inflammatory cytokines such as IL-1β in lung tissue within 96 hours of SARS-CoV-2 infection and no significant increase in serum IL-1β, IL-6 from asymptomatic and mild patients in the early stage of the disease[30,31].

The NLRP3 inflammasome is a common anti-virus immune pathway in response to virus invasion [32]. The NLRP3 inflammasome is mainly composed of NLRP3, ASC, and caspase-1. Upon activation, NLRP3 could assemble with ASC, and the assembly finally activates caspase-1. The activation of caspase-1 plays a key role in IL-1β maturation and cleaves full-length GSDMD into a GSDMD N-terminal fragment and a GSDMD C-terminal fragment, while the cleavage of full-length GSDMD and pore formation is vital for IL-1β release [15,33]. ASC is an adaptor protein containing two domains—pyrin and CARD, which connect upstream

Posted on 24 Jan 2023 — The copyright holder is the author/funder. All rights reserved. No reuse without permission. — https://doi.org/10.22541/au.167458073.32400363/v1 — This a preprint and has not been peer reviewed. Data may be preliminary.

NLRP3 and downstream pro-caspase-1 [34]. The oligomerization of ASC dimers is the key to constituting pyroptosome also called ASC speck [35]. The formation of ASC specks is the symbol of NLRP3 inflammasome activation which recruits pro-caspase-1 to self-catalyze. The activation form of caspase-1 (p20) induces IL-1β maturation and cleaves the full length of GSDMD into GSDMD-N and GSDMD-C. GSDMD-N forms a pore on the membrane that releases IL-1β, and finally, the cell swells to death [20,34]. In this research, we observe that SARS-CoV-2 PLP-TM could decrease the oligomerization of ASC by interacting with ASC, so that the NLRP3 inflammasome pathway is inhibited.

As previous studies show that the transmembrane domains of nsp3 could participate in the formation of double-membrane vesicles (DMVs) and convoluted membranes (CMs) derived from endoplasmic reticulum (ER) infected coronaviruses [5], which might explain why SARS-CoV-2 PLP-TM forms a "ring-like" structural and grabs an ASC speck around. Since SARS-CoV-2 PLP-TM didn't block NLRP3-ASC complex formation but could co-localize with ASC, we speculate that the interaction between SARS-CoV-2 PLP-TM and ASC might block the interaction between ASC and pro-caspase-1, so that the activated form of pro-caspase-1 (p20) was inhibited.

Furthermore, posttranslational modifications like ubiquitination could regulate immune responses, such as IKK activation, MAPK activation, TBK1/IKKε activation, NLR signaling, and so on [36]. Ubiquitination is essential for the oligomerization of ASC[25,26]. In our study, SARS-CoV-2 PLP-TM interacts with ASC and performs a DUB activity that inhibits ASC oligomerization, preventing the formation of NLRP3 complexes and thus blocking the pathway. Then, the maturation of IL-1β is inhibited. Meanwhile, SARS-CoV-2 PLP-TM suppresses the activation of pro-caspase-1, decreasing the cleavage of GSDMD and weakening pyroptosis. Then, the release of IL-1β is also inhibited. As the result, the host cannot produce effective antiviral immunity, which helps the virus escape from the host's antiviral immunity and provides the maximum advantage for the replication of the virus.

Above all, in this research, it was uncovered that SARS CoV-2 papain-like protease inhibits IL-1β maturation and host pyroptosis through disruption of ASC oligomerization and the deubiquitination of ASC, which subsequently negatively regulated the NLRP3 inflammasome pathway. These insights uncover the flex function of CoV encoding proteases. Furthermore, this research may provide a new vision of COVID-19 epidemic prevention and new possibilities for new therapies.

5 Conflict of Interest

The authors declare no potential conflict of interest.

6 Author Contributions

All the authors contributed to the research significantly. Yaling Xing and Yajie Wang conceived and designed the research. Huan Meng performed the experiments and Jianglin Zhou assist with the single-cell RNA sequence reanalysis. All the authors provided critical advice for the revision of the manuscript.

7 Funding

This work was supported by the National Natural Science Foundation of China (grant No.82072285 to Y.Xing)

8 Acknowledgments

We thank Jian Wang at Beijing Proteome Research Center for providing Myc-NLRP3, Myc-ASC, and Myc-pro-caspase-1 plasmids.

Figure legends

FIGURE 1 Analysis of NLRP3 inflammasome pathway based on single-cell transcriptional sequence data in innate immune cells from COVID-19 patients. (A) The expression level of the inflammasome pathway (NLRP3, NLRP6, PYCARD, IL1B, IL18, TRIM31, FBXL2, MARCH7) across four conditions. (B) Expression levels of NLRP3, MARCH7, IL-1β, and IL-18 in innate immune cells from

Posted on 24 Jan 2023 — The copyright holder is the author/funder. All rights reserved. No reuse without permission. — https://doi.org/10.22541/au.167458073.32400363/v1 — This a preprint and has not been peer reviewed. Data may be preliminary.

each group were calculated. The single-cell transcriptional profiling of innate immune cells was gotten from health donors (n=5), SARS-CoV-2-infected moderate patients (n=7), severe patients (n=4), and convalescent (n=6). Wilcoxon rank-sum test was applied to test the significance of the difference between conditions. *P <0.05, ** P <0.01, ***P <0.001, **** P <0.0001.

ΦΙΓΥΡΕ 2 ΣΑΡΣ-δ″-2 ΠΛΠ ινηιβιτς ςασπασε-1 ςλεααγε ανδ ματυρατιον οφ ΙΛ-1β. (A) The plasmids encoding V5/HisB-tagged SARS-CoV-2 PLP-TM or pcDNA3.1 V5/HisB were co-transfected with plasmids encoding Myc-tagged NLRP3, Pro-caspase-1, ASC and plasmids encoding Flag-tagged pro-IL-1β into HEK-293T cells for 24h. Supernatants were collected for an ELISA to determine IL-1β levels and cell lysates were immunoblotted with antibodies against V5, Myc, or Flag. (B) THP-1 macrophages stably expressing Flag-tagged SARS-CoV-2 PLP-TM or control vector were pretreated with 1ug/ml LPS followed with 10μmol/L nigericin for 1.5h. Supernatants were collected for an ELISA to determine IL-1β levels and cell lysates were immunoblotted with antibodies against the indicated proteins. Student's t-test was used and data were shown as means ± SD of three technical replicates. NS, non-significant; *P <0.05.

FIGURE 3 SARS-CoV-2 PLP inhibits GSDMD-N mediated cell pyroptosis.

THP-1 macrophages stably expressing Flag-tagged SARS-CoV-2 PLP-TM or control vector were pretreated with 1ug/ml LPS followed with 10μmol/L nigericin for 1.5h. (A) Cell lysates were immunoblotted with antibodies against the indicated proteins. (B) Cell death was examined by LDH release assay in supernatants. (C) Cell viability was examined by ATP in cell lysates. Student's t-test was used and data were shown as means ± SD of three technical replicates. NS, non-significant, *P <0.05, **P <0.01, ***P <0.001.

FIGURE 4 SARS-CoV-2 PLP partially co-localizes with ASC. (A) HEK-293T cells were transfected with V5-SARS-CoV-2 PLP-TM or Myc-NLRP3 or Myc-pro-caspase-1 or HA-ASC for 24h. The sub-cellular locations of Myc-NLRP3 (red), Myc-pro-caspase-1 (red), HA-ASC (purple), V5-SARS-CoV-2 PLP-TM (green), and nucleus marker DAPI (blue) were visualized with confocal microscopy. (B) HEK-293T cells were transfected with V5-SARS-CoV-2 PLP-TM + Myc-NLRP3 or V5-SARS-CoV-2 PLP-TM + Myc-pro-caspase-1 or V5-SARS-CoV-2 PLP-TM + HA-ASC. Twenty-four hours later, the immunofluorescence assay was performed using a confocal microscope. (C) HEK-293T cells were transfected with GFP-vector or GFP-SARS-CoV-2 PLP-TM or Myc-NLRP3 + HA-ASC or GFP-vector + Myc-NLRP3 + HA-ASC or GFP-SARS-CoV-2-PLP-TM + Myc-NLRP3 + HA-ASC. Twenty-four hours later, the immunofluorescence assay was performed using a confocal microscope. (D) PMA differentiated THP-1 macrophages were stably infected with CT-lentivirus or Flag-SARS-CoV-2 PLP-TM-lentivirus were incubated with PBS or 1ug/ml LPS for 3h plus 10μmol/L Nigericin for 3h. The sub-cellular locations of ASC (red), Flag-SARS-CoV-2 PLP-TM (green), and nucleus marker (blue) were visualized with confocal microscopy. (E) PMA differentiated THP-1 macrophages were stably infected with CT-lentivirus or Flag-SARS-CoV-2 PLP-TM-lentivirus were incubated with PBS or 1ug/ml LPS for 3h plus 10μmol/L Nigericin for 3h. The three-dimensional reconstructions of ASC (red), Flag-SARS-CoV-2 PLP-TM (green), and nucleus marker (blue) were visualized with confocal microscopy.

FIGURE 5 SARS-CoV-2 PLP interacts with ASC. (A) HEK-293T cells were transfected with plasmids encoding Myc-tagged NLRP3 (lanes 3 and 4), or with plasmids encoding V5-tagged SARS CoV-2 PLP-TM (lanes 2 and 4) and with an empty V5-tagged vector. Cell lysates were collected and immunoprecipitated with antibodies against Myc, followed by immunodetection with antibodies against V5. Immunoblot analysis of input was conducted as indicated. (B) HEK-293T cells were transfected with plasmids encoding Myc-tagged pro-caspase-1 (lanes 3 and 4), or with plasmids encoding V5-tagged SARS CoV-2 PLP-TM (lanes 2 and 4) and with an empty V5-tagged vector. Cell lysates were collected and immunoprecipitated with antibodies against Myc, followed by immunodetection with antibodies against V5. Immunoblot analysis of input was conducted as indicated. (C) HEK-293T cells were transfected with plasmids encoding Myc-tagged ASC (lanes 3 and 4), or with plasmids encoding V5-tagged SARS CoV-2 PLP-TM (lanes 2 and 4) and with an empty V5-tagged vector. Cell lysates were collected and immunoprecipitated with antibodies against Myc, followed by immunodetection with antibodies against V5. Immunoblot analysis of input was conducted as indicated. (D) HEK-293T cells were transfected with plasmids encoding Flag-tagged pro-IL-1β

Posted on 24 Jan 2023 — The copyright holder is the author/funder. All rights reserved. No reuse without permission. — https://doi.org/10.22541/au.167458073.32400363/v1 — This a preprint and has not been peer reviewed. Data may be preliminary.

(lanes 3 and 4), or with plasmids encoding V5-tagged SARS CoV-2 PLP-TM (lanes 2 and 4) and with an empty V5-tagged vector. Cell lysates were collected and immunoprecipitated with antibodies against Myc, followed by immunodetection with antibodies against V5. Immunoblot analysis of input was conducted as indicated.

FIGURE 6 SARS-CoV-2 PLP interrupts the oligomerization of ASC.(A) HEK-293T cells were co-transfected with Myc-tagged NLRP3, pro-caspase-1, ASC, and Flag-tagged pro-IL-1β. Cell lysates were collected for immunoblotting analysis of ASC oligomerization. (B) THP-1 macrophages stably expressing Flag-tagged SARS-CoV-2 PLP-TM or control vector were pretreated with 1ug/ml LPS followed with 10μmol/L nigericin for 1.5h. Cell lysates were collected for immunoblotting analysis of ASC oligomerization.

FIGURE 7 SARS-CoV-2 PLP decreases the K63- and K48-linked ubiquitination of ASC. (A) Immunoblot analysis of lysates from HEK-293T cells transfected with Myc-tagged NLRP3, Flag-tagged ubiquitin (Flag-Ub), and V5-tagged SARS-CoV-2 PLP-TM, followed by immunoprecipitation with antibodies against Flag and immunodetection with antibodies against Myc. Immunoblotting of input was detected as indicated. (B) Immunoblot analysis of lysates from HEK-293T cells transfected with HA-tagged ASC, Flag-tagged ubiquitin (Flag-Ub), and V5-tagged SARS-CoV-2 PLP-TM, followed by immunoprecipitation with antibodies against Flag and immunodetection with antibodies against HA. Immunoblotting of input was detected as indicated. (C) Immunoblot analysis of lysates from HEK-293T cells transfected with Myc-tagged pro-caspase-1, Flag-tagged ubiquitin (Flag-Ub), and V5-tagged SARS-CoV-2 PLP-TM, followed by immunoprecipitation with antibodies against Flag and immunodetection with antibodies against Myc. Immunoblotting of input was detected as indicated. (D) Immunoblot analysis of lysates from HEK-293T cells transfected with Flag-tagged ASC, HA-tagged K63-linked ubiquitin, and V5-tagged SARS-CoV-2 PLP-TM, followed by immunoprecipitation with antibodies against Flag and immunodetection with antibodies against HA. Immunoblotting of input was detected as indicated. (E) Immunoblot analysis of lysates from HEK-293T cells transfected with Flag-tagged ASC, HA-tagged K48-linked ubiquitin, and V5-tagged SARS-CoV-2 PLP-TM, followed by immunoprecipitation with antibodies against Flag and immunodetection with antibodies against HA. Immunoblotting of input was detected as indicated. * Non-specific band

FIGURE 8 The hypothetical model describing the mechanisms by which SARS-CoV-2 PLP negatively regulates NLPL3 inflammasome immune pathway and pyroptosis. SARS-CoV-2 PLP-TM interacts with ASC and reduces the K48- and K63-linked ubiquitination of ASC, which decreases the oligomerization of ASC. As a result, SARS-CoV-2 PLP-TM might block IL-1β maturation, and inhibit the activation of GSDMD. Finally, the release of IL-1β is reduced.

FIGURE S1 Identification and annotation of monocytes, dendritic cells, and natural killer (NK) cells from PBMCs of the COVID-19 patients and healthy controls. (A) UMAP representation of identified monocytes, dendritic cells, and NK cells, with every cell colored according to its cell type. (B) UMAP plots show the information of cells' sample origin. Every cell was depicted in a specific color to indicate its original sample information. (C) UMAP projection of the expression levels of canonical markers of $CD14^+$ monocytes (LYZ^+CD14^+), CD16+monocytes ($LYZ^+FCGR3A^+$), monocyte-derived dendritic cells ($CD1C^+$), plasmacytoid dendritic cells ($LILRA4^+$), and NK cells ($KLRF1^+$).

FIGURE S2 The construction of SARS-CoV-2 PLP-TM expressing component. The PLP-TM encoding nucleotide sequence (aa1564-2394 in pp1ab) of SARS-CoV-2 Wuhan-Hu-1 (GenBank accession number NC_045512.2) was synthesized after codon optimization and cloned into pcDNA3.1-V5/HisB plasmid between BamHI and EcoRI.

ΦΙΓΥΡΕ Σ3 ΣΑΡΣ-ô˝-2 ΠΛΠ ινηιβιτς τηε εξπρεσσιον οφ ςασπασε-1 (π20) ανδ ματυρατιον οφ ΙΛ-1β (π17) ιν ΒΕΑΣ-2Β ςελλς. BEAS-2B cells were transfected with V5-vector or V5-SARS-CoV-2 PLP-TM for 24h and stimulated with 1ug/ml LPS for 12h plus 10μmol/L nigericin for 1.5h. Cell lysates were collected for Western blotting.

FIGURE S4 LPS plus nigericin did not induce pyroptosis of BEAS-2B cells significantly. (A) BEAS-2B cells were stimulated with 1ug/ml LPS for 12h plus 10μmol/L nigericin for 3h, 2.5h, 2h, 1.5h, 1h,

Posted on 24 Jan 2023 — The copyright holder is the author/funder. All rights reserved. No reuse without permission. — https://doi.org/10.22541/au.167458073.32400363/v1 — This a preprint and has not been peer reviewed. Data may be preliminary.

and 0.5h. Cell lysates were collected for the detection of GSDMD and GSDMD-N. (B) BEAS-2B cells were transfected with V5-vector or V5-SARS-CoV-2 PLP-TM for 24h and stimulated with 1ug/ml LPS for 12h plus 10μmol/L nigericin for 1.5h. Cell death was examined by LDH release assay in supernatants.

Student's t -test was used and data were shown as means ± SD of three technical replicates. NS, non-significant.

FIGURE S5 SARS-CoV-2 PLP interrupts the oligomerization of ASC in BEAS-2B cells. BEAS-2B cells were transfected with V5-vector or V5-SARS-CoV-2 PLP-TM for 24h and stimulated with 1ug/ml LPS for 12h plus 10μmol/L nigericin for 1.5h. Cell lysates were collected for the detection of ASC oligomerization.

9 References

1. World Health Organization. (2023). Coronavirus disease (COVID-19). https://www.who.int/emergencies/diseases/novel-coronavirus-2019 [Accessed January 4, 2023].

2. Diamond MS, Kanneganti TD. Innate immunity: the first line of defense against SARS-CoV-2. *Nature immunology* . Feb 2022;23(2):165-176. doi:10.1038/s41590-021-01091-0

3. Felsenstein S, Hedrich CM. SARS-CoV-2 infections in children and young people. *Clinical immunology (Orlando, Fla)* . Nov 2020;220:108588. doi:10.1016/j.clim.2020.108588

4. Islamuddin M, Mustfa SA, Ullah S, Omer U, Kato K, Parveen S. Innate Immune Response and Inflammasome Activation During SARS-CoV-2 Infection.*Inflammation* . Oct 2022;45(5):1849-1863. doi:10.1007/s10753-022-01651-y

5. Lei J, Kusov Y, Hilgenfeld R. Nsp3 of coronaviruses: Structures and functions of a large multi-domain protein. *Antiviral research* . Jan 2018;149:58-74. doi:10.1016/j.antiviral.2017.11.001

6. Clementz MA, Chen Z, Banach BS, et al. Deubiquitinating and interferon antagonism activities of coronavirus papain-like proteases.*Journal of Virology* . May 2010;84(9):4619-29. doi:10.1128/jvi.02406-09

7. Sun L, Xing Y, Chen X, et al. Coronavirus papain-like proteases negatively regulate antiviral innate immune response through disruption of STING-mediated signaling. *PloS one* . 2012;7(2):e30802. doi:10.1371/journal.pone.0030802

8. Chen X, Yang X, Zheng Y, Yang Y, Xing Y, Chen Z. SARS coronavirus papain-like protease inhibits the type I interferon signaling pathway through interaction with the STING-TRAF3-TBK1 complex. *Protein & cell* . May 2014;5(5):369-81. doi:10.1007/s13238-014-0026-3

9. Chen X, Wang K, Xing Y, et al. Coronavirus membrane-associated papain-like proteases induce autophagy through interacting with Beclin1 to negatively regulate antiviral innate immunity. *Protein & cell* . Dec 2014;5(12):912-27. doi:10.1007/s13238-014-0104-6

10. Rut W, Lv Z, Zmudzinski M, et al. Activity profiling and crystal structures of inhibitor-bound SARS-CoV-2 papain-like protease: A framework for anti-COVID-19 drug design. *Science advances* . Oct 2020;6(42)doi:10.1126/sciadv.abd4596

11. Gao X, Qin B, Chen P, et al. Crystal structure of SARS-CoV-2 papain-like protease. *Acta pharmaceutica Sinica B* . Jan 2021;11(1):237-245. doi:10.1016/j.apsb.2020.08.014

12. Osipiuk J, Azizi SA, Dvorkin S, et al. Structure of papain-like protease from SARS-CoV-2 and its complexes with non-covalent inhibitors.*Nature communications* . Feb 2 2021;12(1):743. doi:10.1038/s41467-021-21060-3

13. Shin D, Mukherjee R, Grewe D, et al. Papain-like protease regulates SARS-CoV-2 viral spread and innate immunity. *Nature* . Nov 2020;587(7835):657-662. doi:10.1038/s41586-020-2601-5

Posted on 24 Jan 2023 — The copyright holder is the author/funder. All rights reserved. No reuse without permission. — https://doi.org/10.22541/au.167458073.32400363/v1 — This a preprint and has not been peer reviewed. Data may be preliminary.

14. Schroder K, Tschopp J. The inflammasomes. *Cell* . Mar 19 2010;140(6):821-32. doi:10.1016/j.cell.2010.01.040

15. Swanson KV, Deng M, Ting JP. The NLRP3 inflammasome: molecular activation and regulation to therapeutics. *Nature reviews Immunology* . Aug 2019;19(8):477-489. doi:10.1038/s41577-019-0165-0

16. Ren G, Zhang X, Xiao Y, et al. ABRO1 promotes NLRP3 inflammasome activation through regulation of NLRP3 deubiquitination. *The EMBO journal* . Mar 15 2019;38(6)doi:10.15252/embj.2018100376

17. Chen G, Wu D, Guo W, et al. Clinical and immunological features of severe and moderate coronavirus disease 2019. *The Journal of clinical investigation* . May 1 2020;130(5):2620-2629. doi:10.1172/jci137244

18. Harcourt BH, Jukneliene D, Kanjanahaluethai A, et al. Identification of severe acute respiratory syndrome coronavirus replicase products and characterization of papain-like protease activity. *Journal of Virology* . Dec 2004;78(24):13600-12. doi:10.1128/jvi.78.24.13600-13612.2004

19. Kanjanahaluethai A, Chen Z, Jukneliene D, Baker SC. Membrane topology of murine coronavirus replicase nonstructural protein 3. *Virology* . May 10 2007;361(2):391-401. doi:10.1016/j.virol.2006.12.009

20. Burdette BE, Esparza AN, Zhu H, Wang S. Gasdermin D in pyroptosis. *Acta pharmaceutica Sinica B* . Sep 2021;11(9):2768-2782. doi:10.1016/j.apsb.2021.02.006

21. Taabazuing CY, Okondo MC, Bachovchin DA. Pyroptosis and Apoptosis Pathways Engage in Bidirectional Crosstalk in Monocytes and Macrophages. *Cell chemical biology* . Apr 20 2017;24(4):507-514.e4. doi:10.1016/j.chembiol.2017.03.009

22. Wang W, Li G, De W, et al. Zika virus infection induces host inflammatory responses by facilitating NLRP3 inflammasome assembly and interleukin-1β secretion. *Nature communications* . Jan 9 2018;9(1):106. doi:10.1038/s41467-017-02645-3

23. Bryan NB, Dorfleutner A, Rojanasakul Y, Stehlik C. Activation of inflammasomes requires intracellular redistribution of the apoptotic speck-like protein containing a caspase recruitment domain. *Journal of immunology (Baltimore, Md: 1950)* . Mar 1 2009;182(5):3173-82. doi:10.4049/J Immunol.0802367

24. Lin KM, Hu W, Troutman TD, et al. IRAK-1 bypasses priming and directly links TLRs to rapid NLRP3 inflammasome activation. *Proceedings of the National Academy of Sciences of the United States of America* . Jan 14 2014;111(2):775-80. doi:10.1073/pnas.1320294111

25. Guan K, Wei C, Zheng Z, et al. MAVS Promotes Inflammasome Activation by Targeting ASC for K63-Linked Ubiquitination via the E3 Ligase TRAF3. *Journal of immunology (Baltimore, Md: 1950)* . May 15 2015;194(10):4880-90. doi:10.4049/J Immunol.1402851

26. Zhang L, Ko CJ, Li Y, et al. Peli1 facilitates NLRP3 inflammasome activation by mediating ASC ubiquitination. *Cell reports* . Oct 26 2021;37(4):109904. doi:10.1016/j.celrep.2021.109904

27. Klemm T, Ebert G, Calleja DJ, et al. Mechanism and inhibition of the papain-like protease, PLpro, of SARS-CoV-2. *The EMBO journal* . Sep 15 2020;39(18):e106275. doi:10.15252/embj.2020106275

28. Oran DP, Topol EJ. The Proportion of SARS-CoV-2 Infections That Are Asymptomatic: A Systematic Review. *Annals of internal medicine* . May 2021;174(5):655-662. doi:10.7326/m20-6976

29. Yadav R, Chaudhary JK, Jain N, et al. Role of Structural and Non-Structural Proteins and Therapeutic Targets of SARS-CoV-2 for COVID-19. *Cells* . Apr 6 2021;10(4)doi:10.3390/cells10040821

30. Chu H, Chan JF, Wang Y, et al. Comparative Replication and Immune Activation Profiles of SARS-CoV-2 and SARS-CoV in Human Lungs: An Ex Vivo Study With Implications for the Pathogenesis of COVID-19. *Clinical infectious diseases: an official publication of the Infectious Diseases Society of America* . Sep 12 2020;71(6):1400-1409. doi:10.1093/cid/ciaa410

Posted on 24 Jan 2023 — The copyright holder is the author/funder. All rights reserved. No reuse without permission. — https://doi.org/10.22541/au.167458073.32400363/v1 — This a preprint and has not been peer reviewed. Data may be preliminary.

31. Anantharaj A, Gujjar S, Verma N, et al. Resolution of viral load in mild COVID-19 patients is associated with both innate and adaptive immune responses. *Journal of clinical virology: the official publication of the Pan American Society for Clinical Virology* . Jan 2022;146:105060. doi:10.1016/j.jcv.2021.105060

32. Chen N, Xia P, Li S, Zhang T, Wang TT, Zhu J. RNA sensors of the innate immune system and their detection of pathogens. *IUBMB life* . May 2017;69(5):297-304. doi:10.1002/iub.1625

33. Weber ANR, Bittner ZA, Shankar S, et al. Recent insights into the regulatory networks of NLRP3 inflammasome activation. *Journal of cell science* . Dec 3 2020;133(23)doi:10.1242/jcs.248344

34. Zhen Y, Zhang H. NLRP3 Inflammasome and Inflammatory Bowel Disease.*Frontiers in immunology* . 2019;10:276. doi:10.3389/fimmu.2019.00276

35. Fernandes-Alnemri T, Wu J, Yu JW, et al. The pyroptosome: a supramolecular assembly of ASC dimers mediating inflammatory cell death via caspase-1 activation. *Cell death and differentiation* . Sep 2007;14(9):1590-604. doi:10.1038/sj.cdd.4402194

36. Hu H, Sun SC. Ubiquitin signaling in immune responses. *Cell research* . Apr 2016;26(4):457-83. doi:10.1038/cr.2016.40

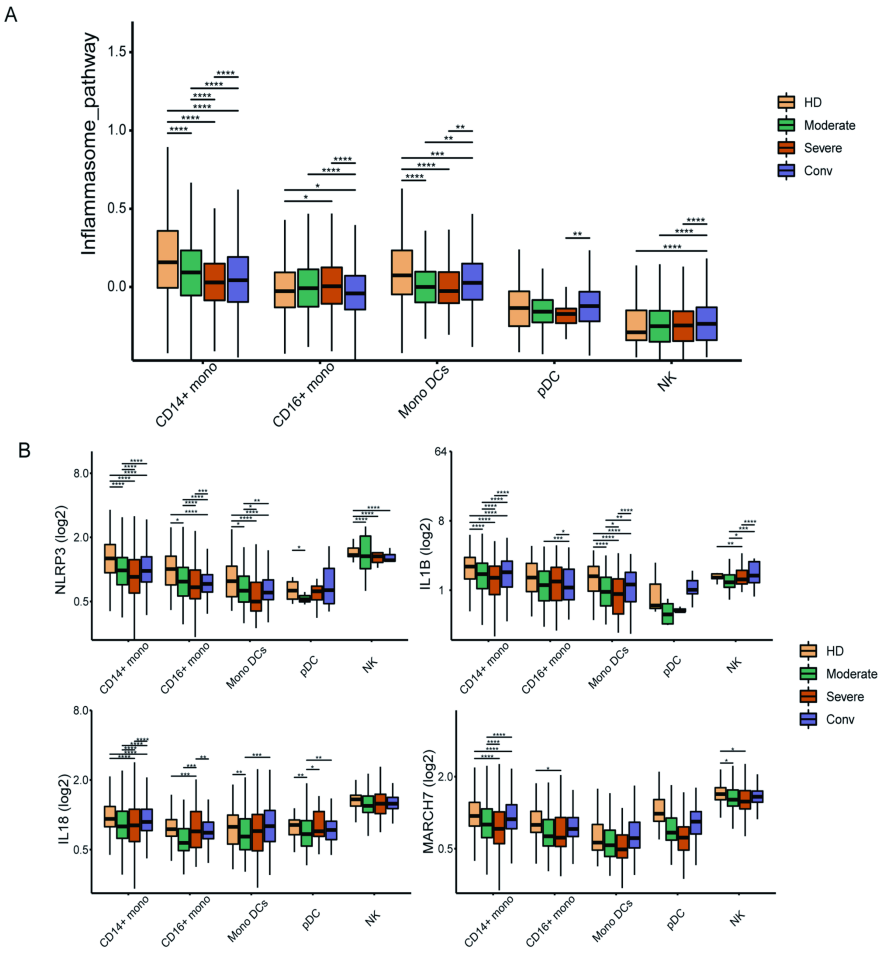

Figure 1

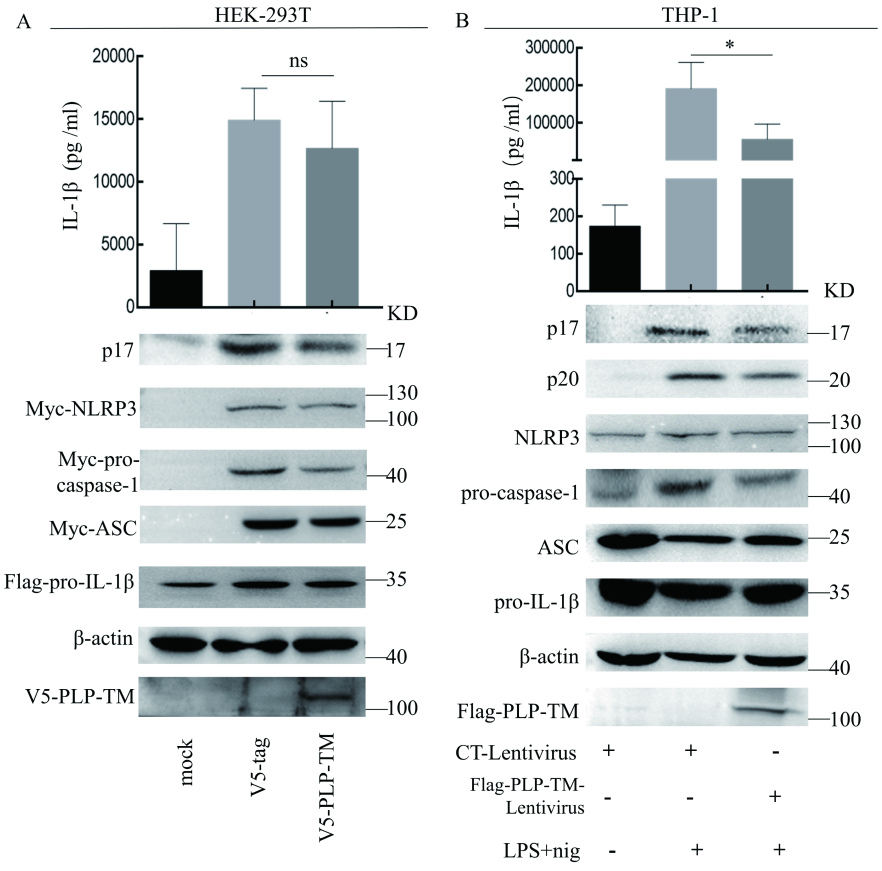

FIGURE.2

Posted on 24 Jan 2023 — The copyright holder is the author/funder. All rights reserved. No reuse without permission. — https://doi.org/10.22541/au.167458073.32400363/v1 — This a preprint and has not been peer reviewed. Data may be preliminary.

Posted on 24 Jan 2023 — The copyright holder is the author/funder. All rights reserved. No reuse without permission. — https://doi.org/10.22541/au.167458073.32400363/v1 — This a preprint and has not been peer reviewed. Data may be preliminary.

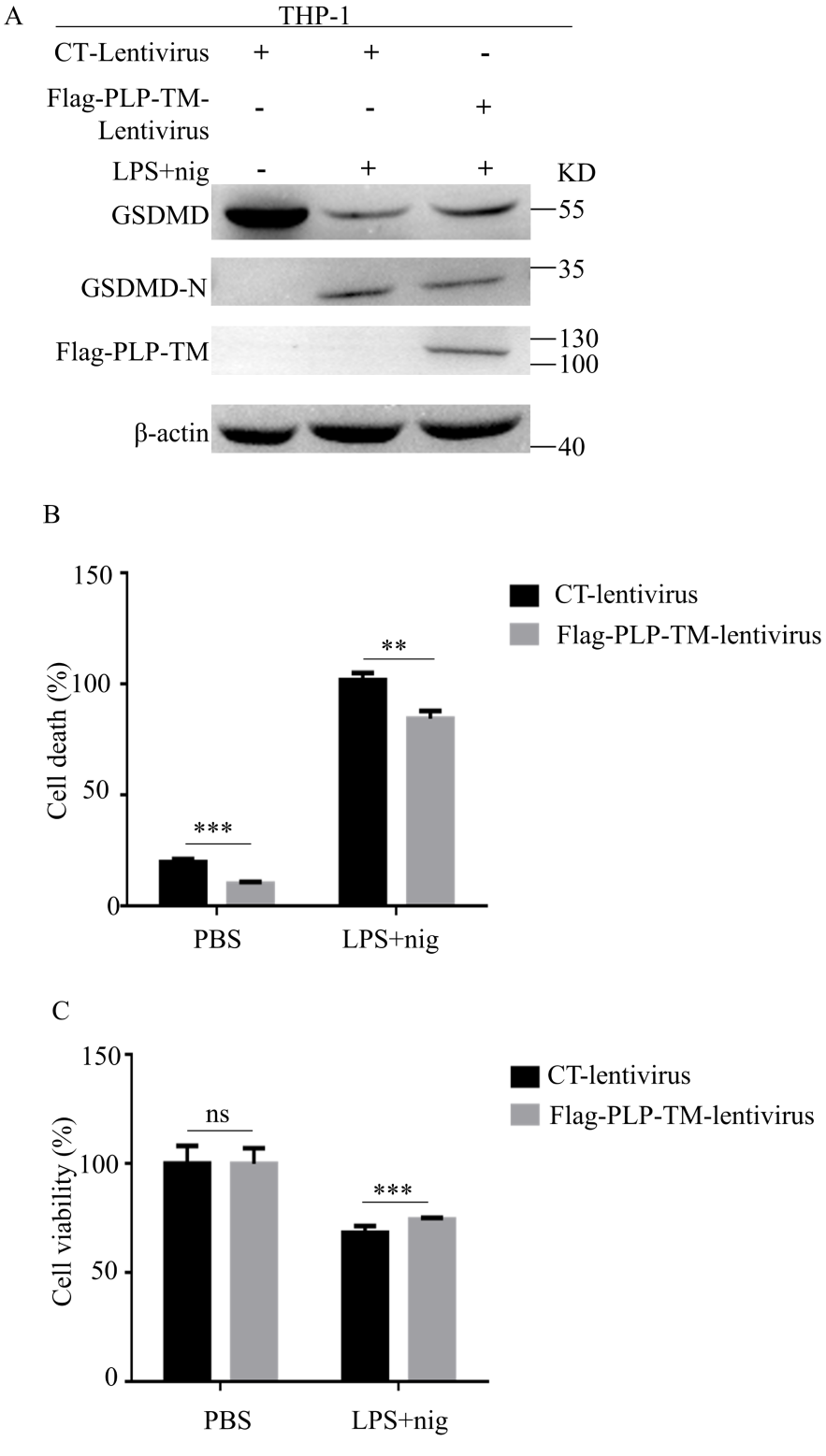

FIGURE.3

Posted on 24 Jan 2023 — The copyright holder is the author/funder. All rights reserved. No reuse without permission. — https://doi.org/10.22541/au.167458073.32400363/v1 — This a preprint and has not been peer reviewed. Data may be preliminary.

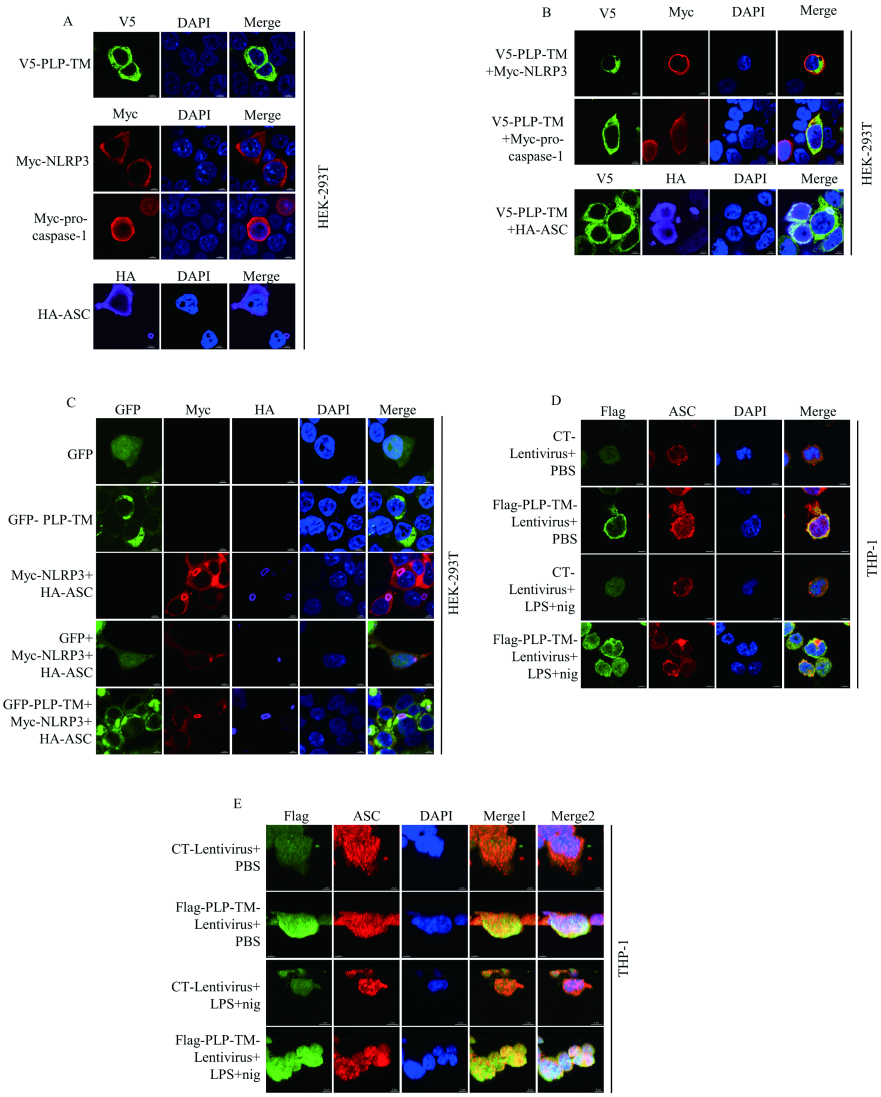

FIGURE.4

Posted on 24 Jan 2023 — The copyright holder is the author/funder. All rights reserved. No reuse without permission. — https://doi.org/10.22541/au.167458073.32400363/v1 — This a preprint and has not been peer reviewed. Data may be preliminary.

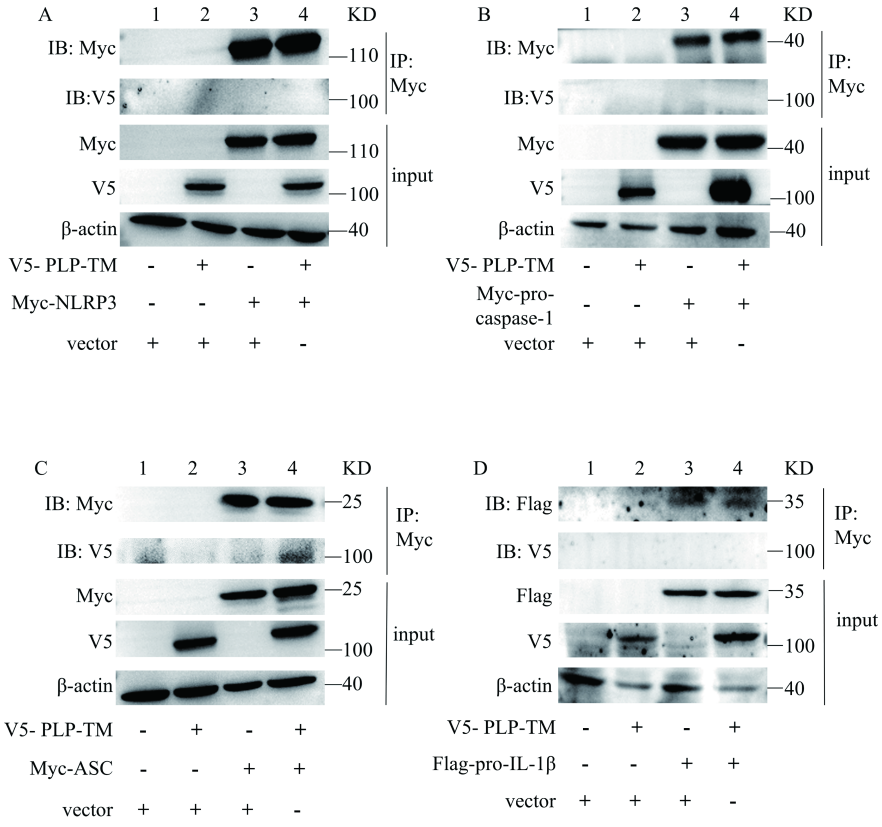

FIGURE.5

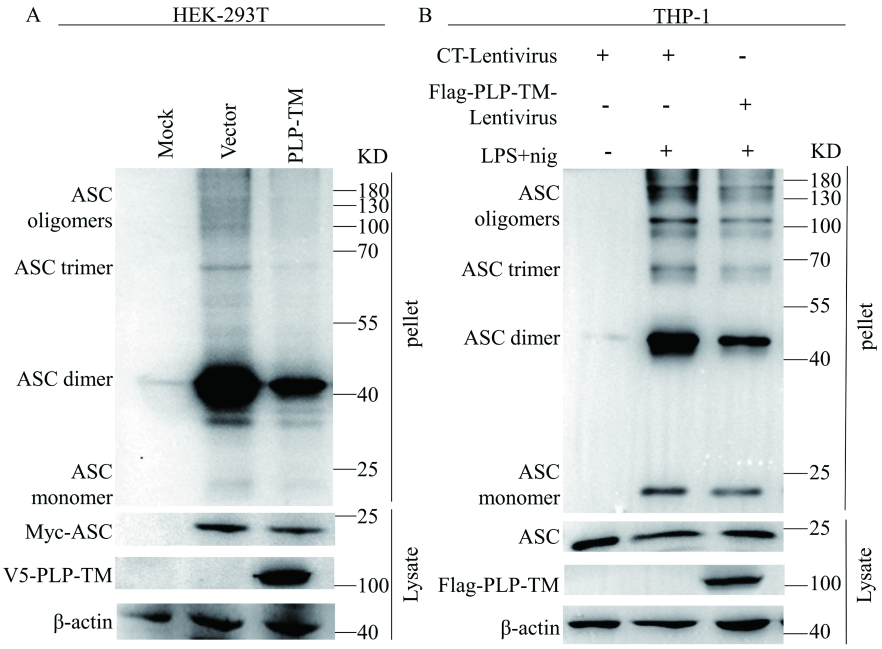

FIGURE.6

Posted on 24 Jan 2023 — The copyright holder is the author/funder. All rights reserved. No reuse without permission. — https://doi.org/10.22541/au.167458073.32400363/v1 — This a preprint and has not been peer reviewed. Data may be preliminary.

Posted on 24 Jan 2023 — The copyright holder is the author/funder. All rights reserved. No reuse without permission. — https://doi.org/10.22541/au.167458073.32400363/v1 — This a preprint and has not been peer reviewed. Data may be preliminary.

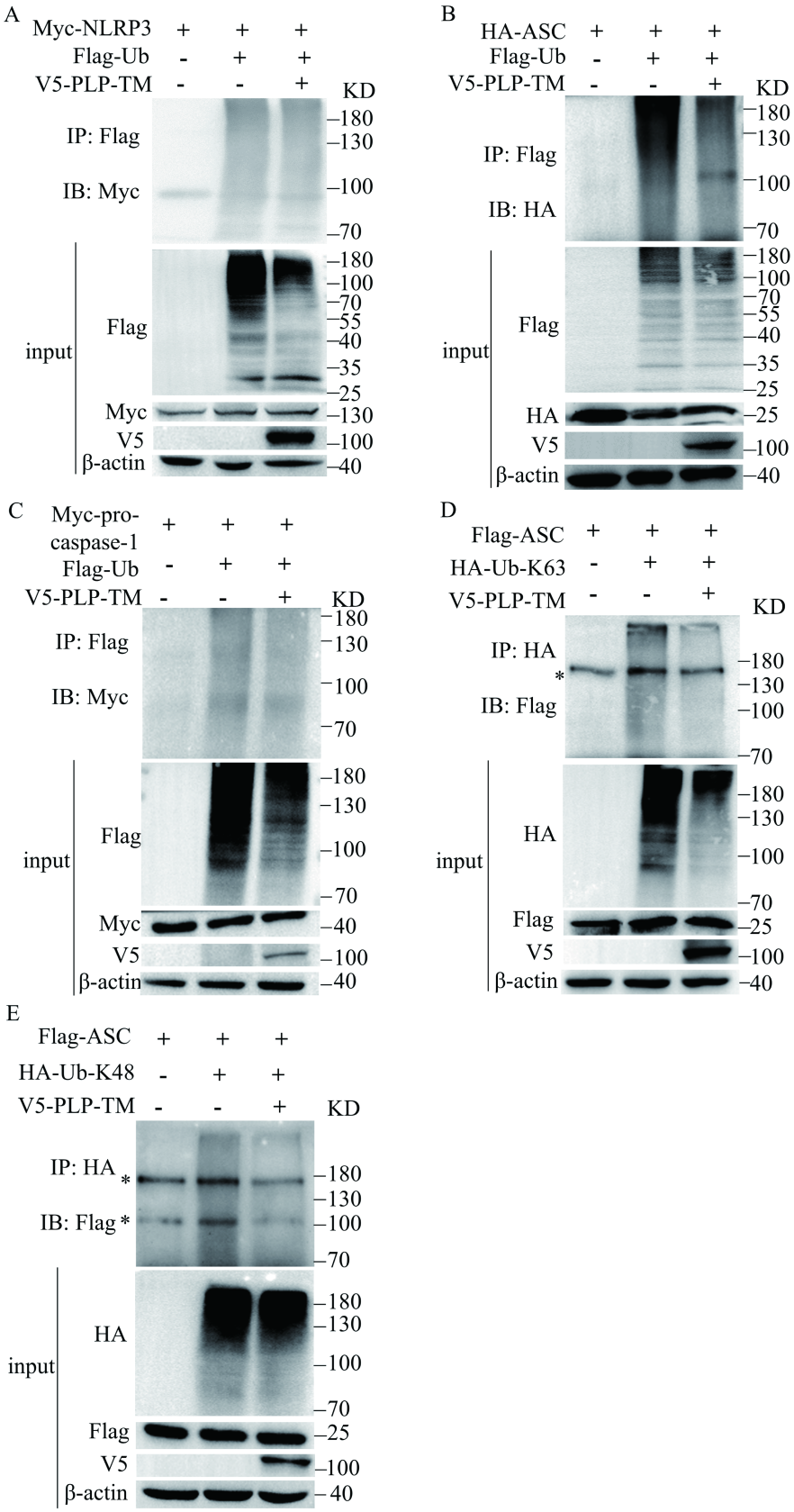

FIGURE.7

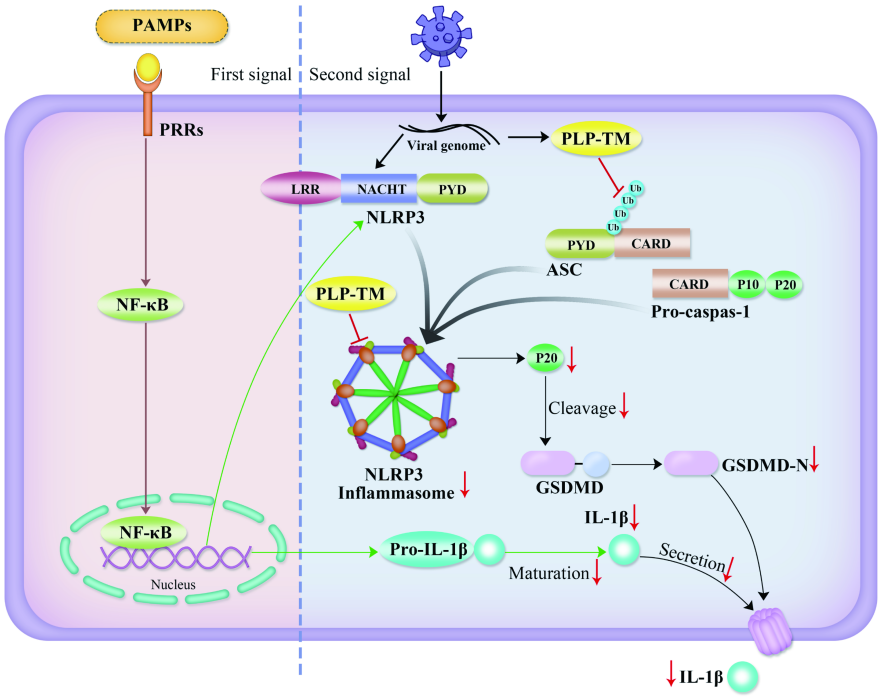

FIGURE. 8

Posted on 24 Jan 2023 — The copyright holder is the author/funder. All rights reserved. No reuse without permission. — https://doi.org/10.22541/au.167458073.32400363/v1 — This a preprint and has not been peer reviewed. Data may be preliminary.